

A02



*Web content*

DAMA collaboration

**Catching Dark Matter Particles  
in the Galactic Halo with DAMA/LIBRA**

*DAMA spokesperson*  
Rita Bernabei

*Collaboration of*  
P. Belli, A. Bussolotti, F. Cappella, V. Caracciolo  
R. Cerulli, C.J. Dai, A. d'Angelo, A. Di Marco  
N. Ferrari, H.L. He, A. Incicchitti, X.H. Ma, A. Mattei  
V. Merlo, F. Montecchia, X.D. Sheng, Z.P. Ye





Aracne editrice

[www.aracneeditrice.it](http://www.aracneeditrice.it)  
[info@aracneeditrice.it](mailto:info@aracneeditrice.it)

Copyright © MMXIX  
Gioacchino Onorati editore S.r.l. – unipersonale

[www.gioacchinoonoratieditore.it](http://www.gioacchinoonoratieditore.it)  
[info@gioacchinoonoratieditore.it](mailto:info@gioacchinoonoratieditore.it)

via Vittorio Veneto, 20  
00020 Canterano (RM)  
(06) 45551463

ISBN 978-88-255-2940-1

*No part of this book may be reproduced  
by print, photoprint, microfilm, microfiche, or any other means,  
without publisher's authorization.*

1<sup>st</sup> edition: December 2019

## VII Preface

### 1 Chapter I

#### *Experimental Evidences and Theoretical Arguments in Favour of Dark Matter*

1.1. Introduction, 1 – 1.2. Mass over Luminosity Ratio in Galactic Systems, 2 – 1.3. The Rotation Curves of Galaxies, 3 – 1.4. Gravitational Lensing, 5 – 1.5. The Bullet Cluster, 8 – 1.6. The Standard Cosmological Model in a Nutshell and Determination of its Parameters, 9 – 1.7. Expansion of the Universe, the Hubble Law and Measurements of the Hubble Constant, 13 – 1.8. The Abundance of the Light Elements and the Primordial Nucleosynthesis, 16 – 1.9. CMB and Baryonic Acoustic Oscillations (BAO), 18 – 1.10. Gravitational Probes, 22 – 1.11. Alternative Hypotheses?, 23 – 1.12. Estimation of some Parameters of the Standard Cosmological Model, 24 – 1.13. What about Dark Matter Features?, 26 – 1.14. Dark Matter in our Galaxy, 26 – 1.15. The Nature of Dark Matter, 29 – 1.16. Mention to DM Candidate Particles, 31 – 1.17. Conclusions, 34.

### 37 Chapter II

#### *Dark Matter Direct Detection: the Signature Strategy*

2.1. Dark Halo Models, 37 – 2.2. The Density and Velocity Distribution of Dark Matter in the Galaxy, 39 – 2.3. A Hypothesis of DM Particle Interaction: the Elastic Scattering, 40 – 2.4. Particle Physics and Nuclear Physics: the Missing Information, Open Problems, 43 – 2.5. A Model Independent Approach: the Annual Modulation Signature in a Nutshell, 45 – 2.5.1. *The DM Annual Modulation Signature in more Detail*, 47 – 2.6. The Annual Modulation on Mars, 52 – 2.7. Data Analysis Exploiting the Annual Modulation Signature, 53 – 2.7.1. *The Residuals*, 57 – 2.7.2. *The Maximum Likelihood Method*, 58 – 2.8. A Connected Second Order Effect: the Diurnal Modulation, 59 – 2.9. Conclusions and Perspectives, 62

### 63 Chapter III

#### *The DAMA/LIBRA set-up*

3.1. The Location: an Underground Site to investigate the Cosmos, 63 – 3.2. The DAMA Project, 65 – 3.3. The DAMA/LIBRA set-up, 66 – 3.4. The Experimental Installation and the Alarm System, 68 – 3.5. The Passive Shield, 72 – 3.5.1. *The Shield from Photons*, 74 – 3.5.2. *The Shield from Neutrons*, 76 – 3.5.3. *The Shield from Radon*, 77 – 3.6. The ULB NaI(Tl) Detectors, 78 – 3.6.1. *Study of Residual Radioactive Contaminants in ULB NaI(Tl) detectors*, 81 – 3.6.2. *Possible Contaminants of Cosmogenic Origin*, 89 – 3.7. Photomultipliers, 93 – 3.7.1. *EMI-*

*Electron Tubes PMTs in DAMA/LIBRA–phase1*, 94 – 3.7.2. *Hamamatsu PMTs with High Quantum Efficiency (QE) in DAMA/LIBRA–phase2*, 96 – 3.8. *The Energy Spectrum at Low Energy* 105 – 3.9. *The Electronic Chain*, 107 – 3.9.1. *The Electronic Chain after the 2008 Upgrade*, 110 – 3.9.2. *The Electronic Chain in DAMA/LIBRA–phase2*, 111 – 3.10. *The Data Acquisition System (DAQ)*, 113 – 3.11. *Conclusions*, 114

## 115 Chapter IV

### *Results from DAMA/LIBRA–phase2 and Combined Analyses*

4.1. *Introduction*, 115 – 4.2. *General Features*, 115 – 4.2.1. *Noise rejection procedures near the software energy threshold*, 115 – 4.2.2. *Total efficiency in the keV energy region and the software energy threshold*, 118 – 4.3. *The Annual Cycles of DAMA/LIBRA–phase2*, 121 – 4.4. *The Annual Modulation of the Residual Counting Rate*, 122 – 4.5. *Absence of Background Modulation*, 125 – 4.6. *The Frequency Analysis*, 129 – 4.7. *Maximum Likelihood Analysis*, 133 – 4.7.1.  *$S_m$  vs  $E$* , 133 – 4.7.2. *Other Analyses on  $S_m$* , 136 – 4.7.3. *Study of the Annual Modulation Phase*, 139 – 4.8. *Further Analysis on Possible Systematics*, 142 – 4.8.1. *The Temperature*, 143 – 4.8.2. *The Radon*, 145 – 4.8.3. *The Noise*, 148 – 4.8.4. *The Calibration Factors*, 149 – 4.8.5. *The Efficiencies*, 151 – 4.8.6. ... *Summarizing*, 152 – 4.9. *No Role for Side Processes in the Results of the Annual Modulation*, 154 – 4.9.1. *No Role for Muons and Fast Neutrons Induced by Muons*, 154 – 4.9.2. *No Role for Environmental Neutrons*, 161 – 4.9.3. *No Role for Solar Neutrinos*, 163 – 4.9.4. *Counting Rate in DAMA/LIBRA Induced by Neutrons, Muons and Solar Neutrinos*, 164 – 4.10. *Few Related Arguments on Comparisons*, 165 – 4.11. *Conclusions*, 166

## 169 *Bibliographic References*

## Catching Dark Matter Particles in Galactic Halo with DAMA/LIBRA



Dark Matter is one of the most challenging topics of contemporary Physics. After a brief introduction to some related general arguments, this book presents the main features of a specific experimental approach in direct detection that could shed light on the nature of Dark Matter. In particular, the main technical aspects and the model independent results achieved with DAMA/LIBRA–phase1 and the first six full annual cycles of DAMA/LIBRA–phase2 are presented. Most of the arguments have already been published in an extensive literature. The aim of this book is to collect all together most of the arguments and to give an overall insight on the model independent results achieved after the pioneer DAMA/NaI experiment focusing on

the strengths of the approach. The obtained model independent evidence is compatible with many different astrophysical, nuclear and particle physics scenarios for Dark Matter particles both inducing nuclear recoils or electromagnetic radiation; this aspect is however out of the discussion in the present book.

The sources of the figures, which do not belong to DAMA works, are quoted in the bibliography at end of the book.

This book is dedicated to the memory of Prof. L. Paoluzi, Director of the INFN–Roma2 at the starting time of the DAMA project, of Prof. D. Prosperi, one of the main proponents of this project, and of Prof. S. d’Angelo who worked in some DAMA activities, and always gave us fruitful scientific and personal support.

DAMA collaboration:

- **R. Bernabei**, Dip. di Fisica, Università degli Studi di Roma “Tor Vergata” and INFN, sez. Roma “Tor Vergata”, Rome, Italy
- **P. Belli**, Dip. di Fisica, Università degli Studi di Roma “Tor Vergata” and INFN, sez. Roma “Tor Vergata”, Rome, Italy
- **A. Bussolotti**, INFN, sez. Roma “Tor Vergata”, Rome, Italy
- **F. Cappella**, Dip. di Fisica, Sapienza – Università di Roma and INFN, sez. Roma, Rome, Italy
- **V. Caracciolo**, INFN Laboratori Nazionali del Gran Sasso, Assergi, Italy
- **R. Cerulli**, Dip. di Fisica, Università degli Studi di Roma “Tor Vergata” and INFN, sez. Roma “Tor Vergata”, Rome, Italy
- **C.J. Dai**, Key Laboratory of Particle Astrophysics, Institute of High Energy Physics, Chinese Academy of Sciences, Beijing, China
- **A. d’Angelo**, Dip. di Fisica, Sapienza – Università di Roma and INFN, sez. Roma, Rome, Italy
- **A. Di Marco**, INFN, sez. Roma “Tor Vergata”, Rome, Italy
- **N. Ferrari**, INFN, sez. Roma “Tor Vergata” and Dip. di Fisica, Sapienza – Università di Roma, Rome, Italy



- **H.L. He**, Key Laboratory of Particle Astrophysics, Institute of High Energy Physics, Chinese Academy of Sciences, Beijing, China
- **A. Incicchitti**, Dip. di Fisica, Sapienza – Università di Roma and INFN, sez. Roma, Rome, Italy
- **X.H. Ma**, Key Laboratory of Particle Astrophysics, Institute of High Energy Physics, Chinese Academy of Sciences, Beijing, China
- **A. Mattei**, INFN, sez. Roma, Rome, Italy
- **V. Merlo**, Dip. di Fisica, Università degli Studi di Roma “Tor Vergata” and INFN, sez. Roma “Tor Vergata”, Rome, Italy
- **F. Montecchia**, INFN, sez. Roma “Tor Vergata” and Dip. Ingegneria Civile e Ingegneria Informatica, Università degli Studi di Roma “Tor Vergata”, Rome, Italy
- **X.D. Sheng**, Key Laboratory of Particle Astrophysics, Institute of High Energy Physics, Chinese Academy of Sciences, Beijing, China
- **Z.P. Ye**, Key Laboratory of Particle Astrophysics, Institute of High Energy Physics, Chinese Academy of Sciences, Beijing, China and University of Jinggangshan, Ji’an, Jiangxi, P.R. China



# Experimental Evidences and Theoretical Arguments in Favour of Dark Matter

## 1.1. Introduction

Since 1687, when the “*Philosophiae Naturalis Principia Mathematica*” by Isaac Newton was published, the motion of astrophysical objects was explained through the Newton's law of gravitation which states that any particle of matter in the Universe attracts any other with a force varying directly as the product of the masses and inversely as the square of the distance between them. Over time, when deviations or anomalies were observed in the experimental data, many in-depth analyses were carried out and contributed to improve our knowledge on gravitation. The presence of irregularities in the motion of planets represents a significant specimen that has allowed revealing the existence of other planets not yet observed, such as Neptune in 1846. Since the beginning of the 1900s, with the new vision of the spacetime offered by the Einstein's special relativity<sup>1</sup> and then by the general relativity<sup>2</sup>, various anomalies have been found in the astrophysical systems from the galactic to the cosmological scale. They have highlighted the existence of a large quantity of non-visible matter, the so-called Dark Matter (DM) in the Universe. At present, Einstein's general relativity is confirmed by all the available experimental tests at astrophysical scale and by some tests available also at cosmological scale. Even more, some experiments performed in laboratory have strongly constrained hypothetical sub-millimetric modification of Newtonian gravity.

<sup>1</sup> It states that the laws of physics are the same for all the non-accelerating observers, and the speed of light in vacuum is independent on the motion of any observer.

<sup>2</sup> It states that a massive object causes a distortion in the spacetime that is perceived as gravity. In this theory gravity can be also a repulsive interaction and not only an attractive force as in the Newton's law.

## 1.2. Mass over Luminosity Ratio in Galactic Systems

The visible mass of an astrophysical object can be empirically estimated from the relationship between its luminosity and the solar one,  $L/L_{\odot}$ , assuming that this ratio is proportional to that of the corresponding masses; on the other hand, the mass of an astrophysical object,  $M$ , can also be estimated through the virial theorem<sup>3</sup>. In 1933 Zwicky, studying the Coma cluster, observed a discrepancy between the visible matter (estimated by its luminosity  $L$ ) and the total matter of the cluster (evaluated by the application of the virial theorem),  $M/L \sim 500$ . He proposed the existence of “*dunkle materie*” (German for “dark matter”) as a source of gravitational potential to explain the rapid motions of the galaxies of the cluster<sup>4</sup>. A similar study was repeated in 1936 by Smith who obtained a similar result for the Virgo cluster:  $M/L \sim 200$ . These observations suggested that most of the galactic and intergalactic matter were not visible. Further observations were carried out in 1939 by Babcock, who studied the  $M/L$  ratio by analysing the rotation speed of the galaxy M31, and in the years 1932–1940 by J.H. Oort, who also analysed other galaxies. Then, Page performed similar studies on double galaxies, obtaining  $M/L$  values of hundreds, and observing for elliptical galaxies  $M/L$  values about 5 times greater than those measured for spiral galaxies.

In the same period (1959), Kahn and Woltjer followed a new approach to study the mass of galaxy systems: by examining the binary system constituted by our Galaxy and the M31 galaxy, they measured the relative motion of the two objects, and derived a mass of the system about 10 times larger than expected from the luminous one. At those times, this “extra mass” was attributed to intergalactic material, but today we explain the anomaly as the measurement of the complete masses of the two galaxies, dark halos included. Subsequently, Rubin, Ford, and Kent (1970) and Roberts and Whitehurst (1975) performed additional studies at Galactic scale (see next section).

<sup>3</sup> It states that, for a stable, self-gravitating, spherical distribution of equal mass objects (stars, galaxies, etc), the total kinetic energy of the objects is equal to minus 1/2 times the total gravitational potential energy, i.e. the potential energy must equal the kinetic energy, within a factor of two.

<sup>4</sup> First attempts to derive the total density of matter in the Solar vicinity were made on 1915–1932, and the term “Dark Matter” was firstly used in 1922 by Kapteyn.

In more recent times the study of the optical and X-ray emission has allowed to determine the temperature and the density of the gas present in the galaxies (mostly hydrogen), through which, assuming that the gas is spherically distributed and in hydrostatic equilibrium, it is possible to trace the profile of the distribution of the baryonic mass inside the cluster itself. The gas density profile can be directly obtained from the X-ray surface brightness, while the temperature can be derived from a spectral analysis. Since the '70s, the orbiting Einstein observatory has carried out analyses of this type, by studying the mass distribution of the Coma, Virgo and Perseo clusters. They have shown that the mass of the hot gas is about 10% of the total mass of the clusters, while the luminous mass is only a fraction of the mass that emits X-rays. Moreover, in galaxy systems, quantitative studies have shown an average  $M/L$  ratio of  $\sim 100$ . More recent analyses were carried out by the ROSAT, XMM-Newton and Chandra experiments, which allowed to determine the density profiles of DM and to measure the total masses of the system even for nearby galaxies. Finally, as in the case of spiral galaxies, the data on elliptical galaxies show a flat profile of the  $M/L$  ratio within an effective radius,  $r_{eff}$ , which then goes up about one order of magnitude at a distance  $\sim 10 \times r_{eff}$ , confirming the presence of DM mainly in galactic halos. In conclusion, there was no doubt that DM is dominant at scales of the galaxy clusters.

### 1.3. The Rotation Curves of Galaxies

After the Second World War the German radar installations were left to an extent in the Netherlands, so Oort and his collaborators decided to use them to study the radio frequency emissions of astrophysical objects. This idea derives from a study by van de Hulst in the 1950s; he calculated that the hydrogen had an emission line at the frequencies of the radio waves (at a wavelength of 21 cm) and pointed out how this radio-emission could allow the measurement of the intergalactic hydrogen speed.

Studies on this radio emission were carried out firstly on our galaxy and then on the M31 galaxy. In particular, the measurements performed on the M31 galaxy showed that hydrogen was present well beyond the luminous region, allowing the study of the rotational curve

of the galaxy up to a distance of  $\approx 30$  kpc<sup>5</sup> from the galactic center. For the first time, this allowed the determination of the  $M/L$  ratio behaviour, as a function of the galactic radius, up to these distances. About ten years later Roberts performed a new study on 21 cm radio emission, to build a mathematical model of the M31 galaxy; the new data were in perfect agreement with those obtained by van de Hulst and collaborators.

In the '70s these studies, combined with those of other groups, led to a crucial result for the evidence of DM. In fact, Rubin and Ford measured the rotation curve of the M31 galaxy by studying its emission in the visible, these data together with those by Roberts and Rots for radio emissions allowed to obtain the rotation curve of the M31 galaxy up to a galactic radius of about 30 kpc. This curve revealed a different trend from that theoretically expected in case of galaxies dominated by visible matter. In fact, at distances between 10 and 30 kpc from the galactic center, the rotation curve of the spiral galaxies exhibited a constant pattern rather than a decreasing trend with increasing distance from the galactic center (see for example the rotational curve of the NGC 6503 spiral galaxy in the Draco constellation reported in Fig. 1.3.1). To explain the behaviour of the orbital circular velocity,  $v_c(r)$ , it is necessary to introduce an additional component of matter, which in this region — called galactic halo — increases the mass,  $M(r)$ , proportionally to the distance from the galactic center,  $r$ . Contrary to the expectations based on the observations of the luminous matter, this points out the existence of collisionless matter with a density profile  $\rho \propto 1/r^2$  at large  $r$ .

Over time, other studies evaluated rotation curves for many spiral galaxies, measuring typically a  $M/L$  ratio, in the peripheral region. In particular, for all the studied spiral galaxies, the flat behaviour of the rotation curves was observed at distance far from the center, supporting with high confidence level the presence of a dark halo. Later on, many experimental data have been collected and rotation curves up to 80–100 kpc have been investigated. In our Milky Way,

<sup>5</sup> Parsec (pc) is the distance to an object whose parallax angle is one arcsecond. It is  $3.085 \times 10^{13}$  km = 3.26 light years.

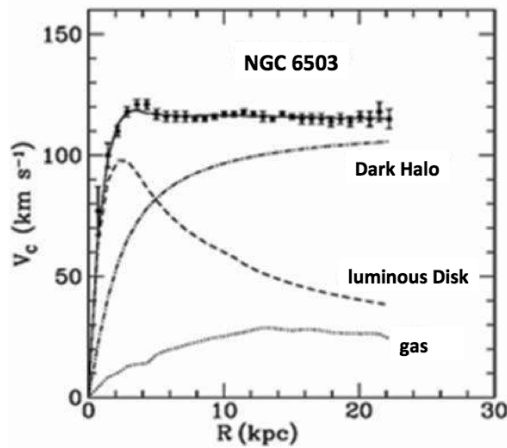


**Figure 1.3.1.** Rotation curve of the NGC 6503 galaxy. The points represent the experimental values. The graph also shows the trends of visible matter, gas and dark matter.

the rotation curve has been studied up to  $\sim 60$  kpc observing  $\sim 2500$  stars by the Sloan Digital Sky Survey (SDSS).

Estimates of the dark halo mass vary in the interval  $(0.6\text{--}3) \times 10^{12} M_{\odot}$ , with solar mass:  $M_{\odot} = 1.99 \times 10^{30}$  kg. The behaviour of the rotation velocity of galaxies as a function of the galactic radius is certainly a decisive evidence for the existence of DM in the galactic halos.

#### 1.4. Gravitational Lensing

The galaxies and clusters, being very massive, generate gravitational fields so high as to be able to significantly deflect the photons emitted from distant objects (stars, quasars, galaxies) placed behind them. Due to the gravitational field and the relative geometry of the space-time, the photons follow the geodesic path that is no more linear as in the euclidean geometry (i.e. far from the gravitational field). This deflection and delay of light, by a gravitational field, produces a distortion of the image of the source that has emitted such photons (some examples and a schema are shown in Fig. 1.4.1).

This phenomenon is called gravitational lensing because the massive objects act on light just like lenses.

Gravitational lensing was predicted by Mitchell (in 1784) and Soldner (in 1801) in the context of Newtonian theory and then derived by Einstein, firstly in 1911 by using the Equivalence principle and the Euclidean metric, and secondly in 1915 by general relativity. In 1919, Eddington and collaborators measured the positions of stars near the Sun, and confirmed Einstein's predictions.

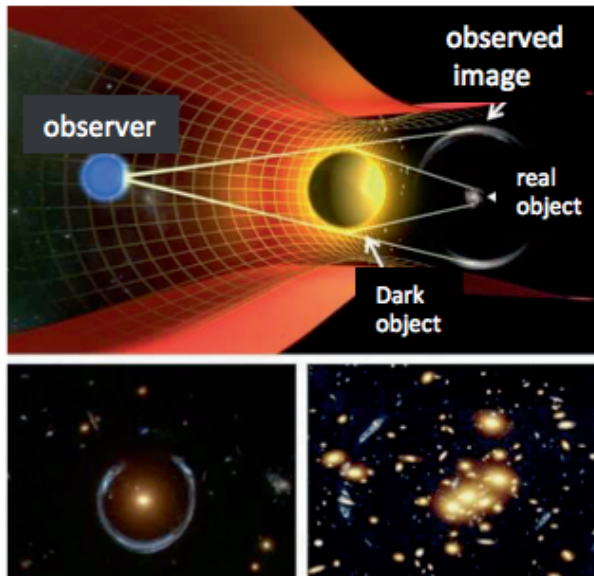


**Figure 1.4.1.** Top: the diagram of the gravitational lensing effect in which a source (real object) emits photons. They travel along the geodesics to the observer and the resulting image of the emitter is diffused/distorted (observed image). Bottom: examples of observation of lensing effect such as distortion with multiple image production (right) and the effect called Einstein ring (left) typical in case of strong lensing.

Gravitational lensing can be:

- strong lensing: multiple images of the source are formed (Einstein's rings, arcs) because the source passes inside the Einstein radius<sup>6</sup> and the images are strongly distorted;

<sup>6</sup> It is a characteristic angle in lens theory and, therefore, has an important role in micro-lensing. It defines a typical scale for separation between multiple images.



- weak lensing: it is the effect on the sources outside the Einstein radius, which are weak lensed. The signal on an individual galaxy is smaller, so an average on many galaxies is needed;
- micro-lensing: it is the lensing by stars (micro-arcsecond scale) with a magnification of background sources. The light intensity varies with time.

The gravitational lensing has improved our knowledge on mass distribution/DM contributions in galaxies/clusters (see Fig. 1.4.2, and examples in sections 1.5., 1.10. and 1.15.).

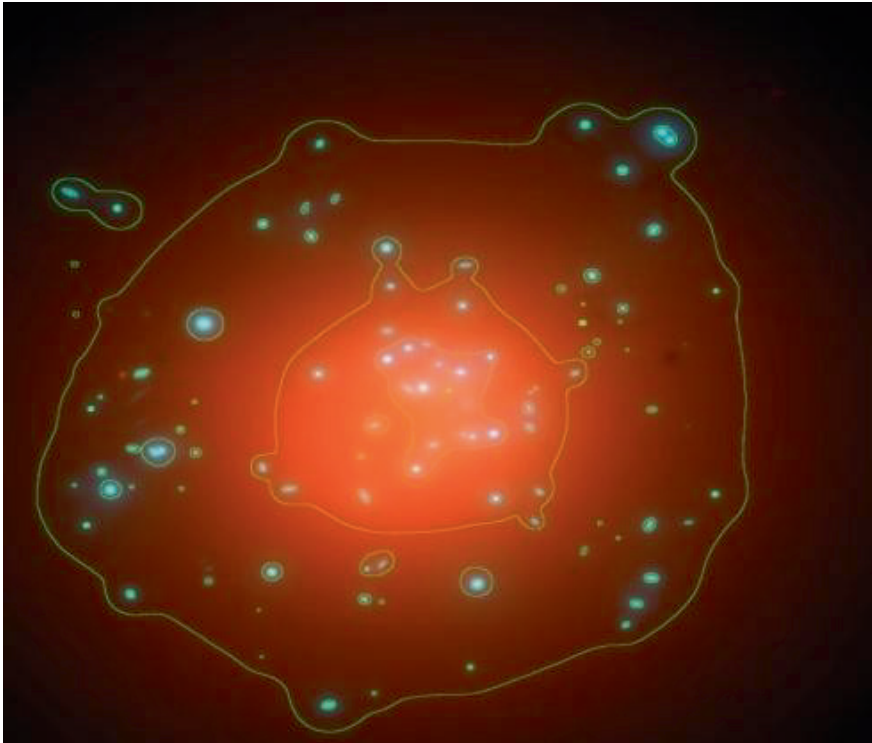


**Figure 1.4.2.** Total mass density map in CL0024 cluster, with luminous matter (blue) and DM (red) contributions.

## 1.5. The Bullet Cluster

The study of the Bullet Cluster (1E 0657–558) represents a direct empirical proof of the existence of DM given by the astrophysics sector. This object consisted of a collision between two galaxy clusters that occurred about 100 million years ago. The name refers to the smaller cluster that moves away from the larger one as a projectile. This collision has been studied through three different types of instruments:

- optical telescope: through telescope observations a mapping of the visible stars in the two clusters was obtained;
- X-rays: through the study of X-rays, a baryon gas mapping has been obtained; this gas constitutes the majority of baryonic matter in the clusters;
- gravitational lensing: the study of gravitational lensing allowed obtaining a mapping of the total mass distribution of the two clusters.

During the collision, components behaving differently in the two clusters (see Fig. 1.5.1) were observed. In particular the baryonic gas and the visible stars of the two clusters, which interact electromag-

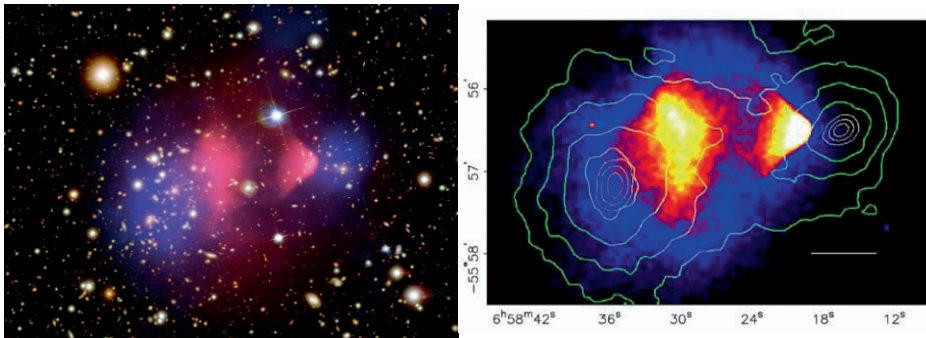


**Figure 1.5.1.** On the left the image is a Hubble/Chandra/Magellan composite with red depicting the X-rays emitted by hot gas, blue depicting the dark matter distribution and white the optical regime; on the right there is a reconstruction of the mass isodensity regions of the Bullet Cluster (green lines) superimposed on the distribution of the X-emitter gas.

netically, are deformed. On the other hand, from gravitational lensing, it is observed that the greater part of the matter of the two clusters is not affected by the impact and is separated from the baryonic component. This observation supports the existence of a dominant component of non-baryonic DM in the two clusters.

In conclusion, the baryonic gas represents the most of the ordinary matter present in the two clusters, while the DM constitutes the dominant component of the total matter in the two clusters. After the collision, it appears well separated from the baryonic gas and not affected by the collision (see Fig. 1.5.1). This clear separation should be absent if the DM had been dominated by a baryonic component. This study has therefore shown that the dominant mass contribution in the two clusters is in the form of non-baryonic and non-collisional DM. The Bullet Cluster is one of the most important direct astrophysical evidence of the existence of the DM.

## **1.6. The Standard Cosmological Model in a Nutshell and Determination of its Parameters**

The evidence of DM, so far reported, concerns observations on a galactic or galaxy cluster scale. In this section a brief overview of the Standard Cosmological Model and the main evidence of DM on a cosmological scale will be resumed.

The Standard Cosmological Model allows explaining some characteristics of the Universe such as the cosmic microwave background radiation (CMB), the abundance of light elements, the large-scale structures. It is based on the Big Bang scenario, according to which the Universe originated about  $10^{10}$  years ago from a highly compressed initial singularity, and on the following theoretical bases:

- the Einstein equations, which bind the geometry of the Universe to its matter/energy content;
- the Cosmological Principle according to which the Universe is spatially homogeneous and isotropic at large scale;
- the Robertson–Walker metric<sup>7</sup> that describes the model.

<sup>7</sup> It is a 4D metric that includes the space–time curvature. It assumes the homogeneity and isotropy of the space, and that the spatial component of the metric can be time–dependent.

The Einstein field equations on which the model is based are (in the Einstein sign convention):

$$R_{\mu\nu} - \frac{1}{2}g_{\mu\nu}R = -\frac{8\pi G}{c^4}T_{\mu\nu} + \Lambda g_{\mu\nu}, \quad (1.6.1)$$

where:  $R_{\mu\nu}$  and  $R$  are, respectively, the tensor and the scalar of Ricci;  $g_{\mu\nu}$  is the metric tensor;  $G$  the universal gravitational constant;  $T_{\mu\nu}$  is the energy–impulse tensor and  $\Lambda$  is the so–called cosmological constant. This equation describes the relationship between matter/energy in the Universe (right–hand terms) with the geometry of the Universe (left–hand terms). In this scenario the cosmological constant  $\Lambda$  can represent a sort of vacuum energy (sometimes associated with the Dark Energy; see later). For the sake of completeness, it is worth to mention that this term was initially inserted by Einstein to obtain static solutions of the equation (1.6.1), but then eliminated after the discovery of the Hubble–Lemaitre expansion and later on reconsidered when the role of Dark Energy was pointed out. Using the Robertson–Walker metric, Einstein's equations lead to the Friedmann equations ( $c=1$ , hereafter):

$$H^2 = \left(\frac{\dot{a}}{a}\right)^2 = \frac{8\pi G}{3}\rho_{tot} - \frac{k}{a^2} + \frac{\Lambda}{3}, \quad (1.6.2)$$

$$\frac{\ddot{a}}{a} = -\frac{4\pi G}{3}(\rho_{tot} + 3p) + \frac{\Lambda}{3}, \quad (1.6.3)$$

where  $H$  is the Hubble variable,  $a$  is the scale factor of the Universe,  $\rho_{tot}$  is the total energy/matter density in the Universe,  $k$  represents the curvature of the Universe, and  $p$  is the pressure.

The geometry of the Universe is given by the metric curvature  $k$ ; in case of  $k = 0$  and  $\Lambda = 0$ , it is possible to define a critical density:

$$\rho_c = \frac{3H^2}{8\pi G} \approx 0.5 \times 10^{-5} \frac{GeV}{cm^3} \approx 10^{-29} \frac{g}{cm^3}, \quad (1.6.4)$$

which corresponds to 6 protons per cubic meter. In particular, the abundance  $\Omega_x$  of a form  $x$ , of energy/matter in the Universe, can be expressed in units of  $\rho_c$ , as: